

# 7 Materials and Technology

## 7.1 OVERVIEW

Many of our activities in the fields of fusion technology and fusion materials development are summarised in this chapter. Those specifically relating to JET and ITER systems are described in Chapters 3, 4 and 8, so this chapter is focussed on the other activities needed to bring fusion power to practical fruition, especially on an accelerated timescale – the development of materials suitable for attractive power plants, the conceptual design of demonstration power plants and analyses of the economic, safety and environmental attributes of fusion power. Much of the work has been undertaken in collaboration with UK universities and almost all of it as part of joint programmes with other Fusion Associations within the European Fusion Development Agreement (EFDA).

## 7.2 MATERIALS MODELLING AND VALIDATION

In 2008/09 materials modelling and validation continued progressing within the framework of two equally significant projects: (i) the EFDA fusion materials programme; and (ii) fusion-relevant materials research funded by EPSRC in UK universities. As the latter, involving several UK universities, and led by the University of Oxford, comes to a close, the materials modelling work at Culham re-focuses. The emphasis of activity at Culham is now on the interpretation of observations, and other information, accumulated by the experimental groups at Oxford, on the development of UK and international collaborations needed for the successful continuation of the Culham programme, and on the development of a range of modelling techniques and methods required for assessing the performance of materials, especially reduced activation steels, in the environment of a fusion power plant.

The UKAEA Culham group has contributed extensively to planning the EFDA programme, both in terms of chairing and managing the work of materials topical group, and through the development of strategy for the future, as formulated in a recent EFDA report on 'Strategic Objectives for Fusion Materials Modelling and Experimental Validation'.

The UKAEA Culham group has also made extensive practical contributions to the EFDA programme in 2008/09. These included the development of techniques for modelling high-temperature properties of iron and steels, and for modelling phase stability of binary Fe-Cr alloys in the high-temperature limit. Significant progress has been achieved in understanding the properties of a class of fundamental line defects characterizing body-centred cubic metals, the so-called screw dislocations (see Figure 7.1); understanding how defects are formed and develop is essential to understanding how rapidly neutrons in fusion reactors will damage and degrade the properties of structural materials.

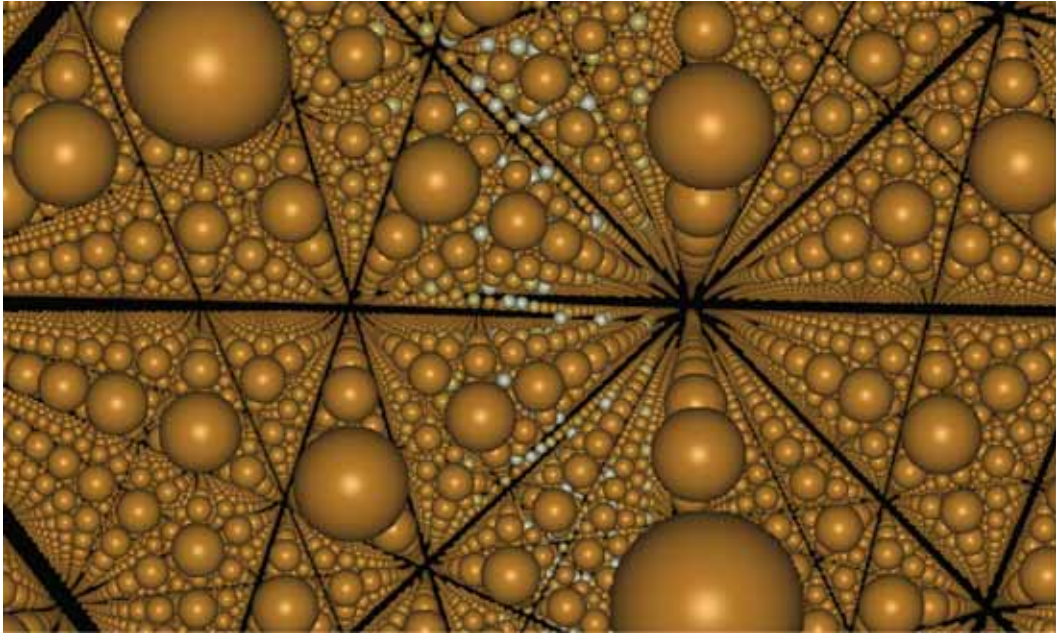


**Figure 7.1:** Atomic structure of a screw dislocation in body-centred cubic iron. Atoms in the core of a dislocation, seen in the centre of the image, are shown in lighter colour. A screw dislocation is a line topological defect, thermally activated migration of which determines whether the response of a material to time-dependent loading is ductile or brittle

Thermally activated Arrhenius migration of screw dislocations determines the temperature of the brittle-ductile transition. This conclusion follows from extensive theoretical investigations of the problem performed in the past, and it agrees with experimental observations performed recently at Oxford within the framework of an experimental programme supported by UKAEA. Observations illustrated by the Arrhenius plot in Figure 7.2 show that the temperature of the brittle-ductile transition, which is one of the main engineering parameter characterizing ferritic steels, alloys, tungsten, vanadium, and other bcc transition metals, varies systematically as a function of the applied strain rate. A material fails in a brittle way if a crack, nucleated or already present in the material, is able to propagate faster than the material is able to accommodate and relax the associated strains and stresses. The relaxation of stress at the crack tip involves mobile defects and dislocations moving away from the crack. In this process the screw dislocations represent the ‘rate limiting’ group of defects. The characteristic activation energy for the ductile-brittle transition found experimentally in pure metals (see Figure 7.2) equals approximately one half of the formation energy for a double kink on a screw dislocation.

Work at Culham has focused on resolving one of the long outstanding problems in modelling screw dislocations, related to the so-called non-degenerate structure of their core. Knowing the structure of the core is a necessary pre-condition for developing a model for a double kink and evaluating the activation energy for the ductile-brittle transition.

Ab initio calculations performed using small simulation cells show that the structure of the core of a screw dislocation is non-degenerate. At the same time, large-scale atomistic simulations carried out using the available simplified interatomic interaction laws often predict symmetry-broken core configurations. Until now, no systematic way of linking the observed structure of the core of a screw dislocation with the assumed form of interatomic interaction law was found. Researchers at Culham, by combining density functional calculations with atomistic simulations, and with the so-called multistring Frenkel-Kontorova model, showed that the occurrence of a non-degenerate screw dislocation core was

related to a particular feature (in effect, the 'shape') of the assumed interatomic interaction law. This finding has now been verified and confirmed by colleagues at the Paul Scherrer Institute, Switzerland. Further analysis has made it possible to formulate a new approach to the derivation of interatomic interaction laws that guarantee the correct structure of the screw dislocation core in atomistic simulations. The Culham work has in this way made a significant step towards the development of a predictive model for a brittle-ductile transition in iron, ferritic steels, and other body-centred cubic metals and alloys.

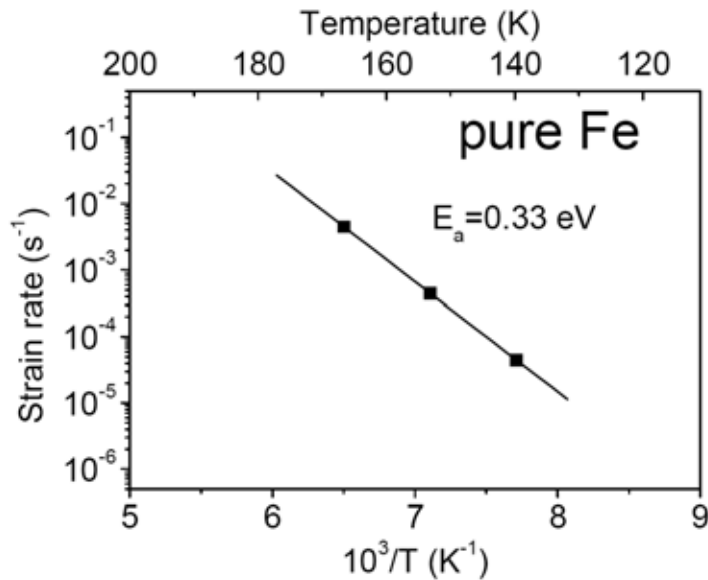


**Figure 7.2:** An Arrhenius plot for the behaviour of the Ductile-Brittle Transition Temperature (DBTT) as a function of applied strain rate. The squares indicate the temperature at which brittle failure occurs (DBTT) for a given strain rate. This plot for iron confirms that the occurrence of ductile-brittle transition is controlled by thermally activated mobility of screw dislocations. This work was performed as a part of experimental programme supported by the UKAEA Fusion Association (figure courtesy of S.G. Roberts, University of Oxford)

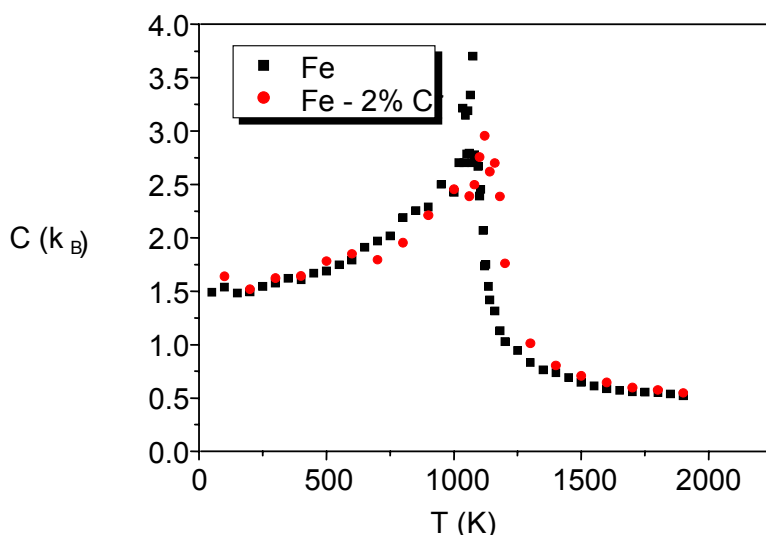


**Figure 7.3:** A characteristic anomaly in the specific heat of iron and Fe-Cr alloys occurring near the Curie temperature of the materials. The behaviour illustrated in the figure was predicted by ab-initio-based magnetic cluster expansion (MCE) Monte-Carlo approach. The Curie temperature  $T_C$  predicted for pure iron is  $\sim 1,100$  K. This value agrees well with the experimentally observed Curie temperature of iron  $T_C = 1,043$  K ( $770^\circ$  C). This figure also shows that the addition of a small amount of chromium raises the Curie temperature. Note that the further increase of chromium concentration to 20% **lowers** the Curie temperature to approximately  $600^\circ$  C

The earlier work on magnetic interatomic potentials, which was followed by the development of spin-lattice dynamics (in collaboration with Hong Kong Polytechnic University), has led to understanding the role played by high-temperature magnetic fluctuations, and the fundamental significance of these fluctuations for modelling such common engineering materials as structural steels, especially in the high-temperature limit. This understanding has led to the development of a new approach to Monte Carlo modelling of magnetic alloys, including Fe-Cr alloys, the so-called Magnetic Cluster Expansion (MCE). In the MCE the energy of an alloy configuration is described by a Hamiltonian that depends not only on the positions of Fe and Cr atoms in the lattice, as in conventional cluster expansion, but also on the configuration of atomic magnetic moments, allowing transpositions and exchange between the former, and relaxations of the latter. Figure 7.3 gives an example of application of the MCE, which shows that the method does give an accurate description of magnetic phase transitions in pure iron and dilute Fe-Cr alloys. The characteristic curve describing fluctuations of magnetic moments at elevated temperatures is a phenomenon that has a direct bearing on fusion plasma confinement technology. Indeed, ferritic steels, which are strongly ferromagnetic at room temperature, become paramagnetic at elevated temperatures close to the operating temperature of a fusion power plant. The proximity of the transition temperature, known as the Curie temperature, of ferritic steels to the range of operating temperatures of a fusion power plant (400-600°C) represents a challenge for plasma confinement technology.

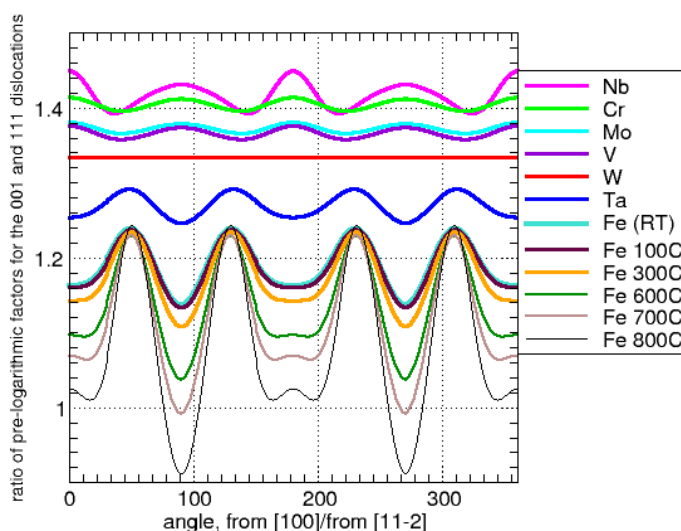


**Figure 7.4:** Ratio of pre-logarithmic factors in the expression for free energy for straight  $\mathbf{b}=a\langle 001 \rangle$  and  $\mathbf{b}=a/2\langle 111 \rangle$  edge dislocations evaluated, in the anisotropic elasticity approximation, for several bcc metals. In the isotropic elasticity approximation this ratio is independent of the orientation of the tangent vector of the dislocation line and equals  $4/3$ . For tungsten, which is nearly elastically isotropic, this ratio is very close to  $4/3 = 1.333$

In describing the orientation of dislocations forming the sides of a loop, the Burgers vector ( $\mathbf{b}$ ) is used. The vector in the  $\langle 001 \rangle$  direction is normal to the face of a bcc cell. The frequent occurrence of  $\mathbf{b}=\langle 001 \rangle$  prismatic edge dislocation loops in body-centred cubic lattice (bcc) iron and iron-based alloys irradiated at high temperatures is one of the most surprising phenomena in the field of radiation damage of materials. It is very unusual that the  $\langle 001 \rangle$  loops form at all, since there is an alternative  $\mathbf{b}=a/2\langle 111 \rangle$  dislocation loop configuration that, according to the conventional isotropic treatment of elasticity, has a lower self-energy (the  $\langle 111 \rangle$  direction being parallel to the long diagonal of the bcc cell).

Work performed at Culham in collaboration with Swiss colleagues showed that this high-temperature radiation damage anomaly has a magnetic origin. More generally, magnetism has important implications for the structural stability of iron-based alloys and steels. The equilibrium atomic structure of a material depends sensitively on magnetic ordering in the case where the magnetic energy and the difference between energies of competing phases are comparable. For example, Hasegawa and Pettifor proved that magnetism stabilizes the body-centred cubic (bcc)  $\alpha$ -phase of iron at low temperatures. This assertion has been fully confirmed by density functional calculations showing that the energy per atom in the non-magnetic or in the antiferromagnetic bcc phases of iron is higher than the energy of any of the face-centred cubic (fcc) phases.

Thermal magnetic fluctuations are responsible for the phase transition from the bcc to the fcc phase occurring approximately at 912° C. As a precursor for this structural phase transformation, iron and iron-based alloys exhibit gradual softening of one of the anisotropic stiffness constants of the material  $c'=(c_{11}-c_{12})/2$ .<sup>1</sup> This constant describes the stiffness of the material along an axis perpendicular to a plane in which compression forces are applied at the four faces of the cube whose centres lie in that plane, the compression being such that the volume of the cube is conserved. According to experimental measurements,  $c'$  decreases by a factor of three between room temperature and 800° C. Such a strong variation of  $c'$  affects interaction between dislocations, as well as the self-energies of dislocation loops in iron and iron-based alloys. Figure 7.4 illustrates a profound effect of temperature on the pre-logarithmic part of the relative free energies of the  $\langle 001 \rangle$  and  $\frac{1}{2}\langle 111 \rangle$  edge dislocations. The curves describing bcc iron show that at ~700° C the ratio of the  $\langle 100 \rangle$  to  $\frac{1}{2}\langle 111 \rangle$  dislocation free self-energies drops below unity, making it *free*-energetically favourable for the low-temperature dislocation configurations of the  $\frac{1}{2}\langle 111 \rangle$  type to convert into a high-temperature  $\langle 100 \rangle$ -type configuration. This modelling prediction has now been fully confirmed by direct *in-situ* electron microscope observations of dislocations loops in iron formed under irradiation at high temperatures.

The strong temperature variation of anisotropic stiffness constants of iron and iron-based alloys not only has a dramatic effect on the self-energies of dislocation loops. Interaction between individual line dislocations is described by laws that are very similar to those determining the free self-energy of dislocation loops. Since interaction between dislocations is what determines the mechanical strength of a crystalline material, work at Culham is presently focusing on understanding fundamentals of interaction between dislocations in the high temperature limit.

One of the examples illustrating the effect of anisotropic elastic interactions on high-temperature strength is the problem of dislocation pile-ups. Pile-ups form if an ensemble of mobile dislocations is impeded by an obstacle, for example by an oxide particle in oxide dispersion strengthened (ODS) steel. Figure 7.5 illustrates the universal character of dislocation pile-ups containing various numbers of dislocations. As the strength of interaction between individual dislocations in the pile-up decreases (for example, in iron at high temperature), dislocation sources generate more dislocations, in this way accelerating plastic deformation of the material.

Figure 7.6 shows electron microscope images of pure iron deformed at two different temperatures. Experimental observations show that dislocation pile-ups formed at higher temperatures are more compact, and that they contain many

<sup>1</sup> The other two constants are the bulk modulus (B) and the stiffness constant  $c_{44}$

more dislocation lines, in agreement with the solution of the problem of interacting dislocations in a pile-up.

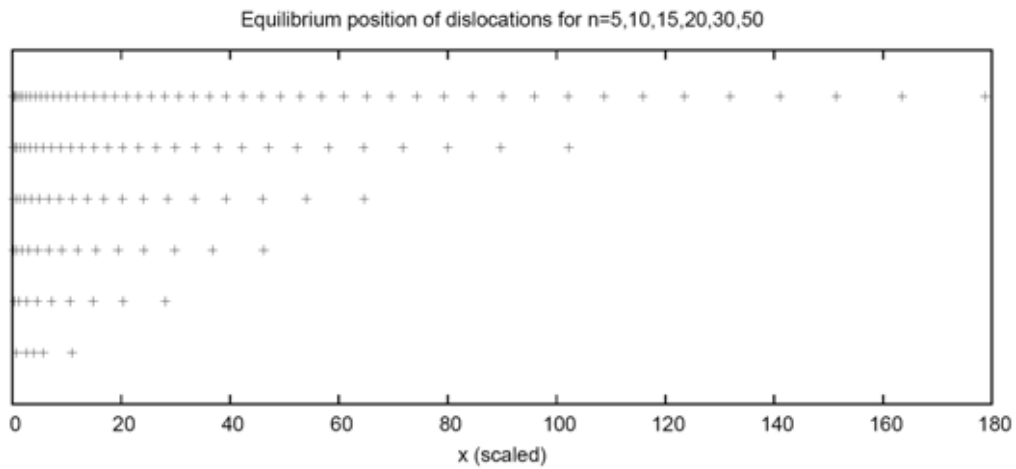


**Figure 7.5:** Sketch illustrating the universal structure of pile-ups formed by edge dislocations if one of the dislocations in the pile-up is pinned by an obstacle. Although this one-dimensional model is an idealization, it still illustrates the qualitative behaviour exhibited by mesoscopic ensembles of dislocations

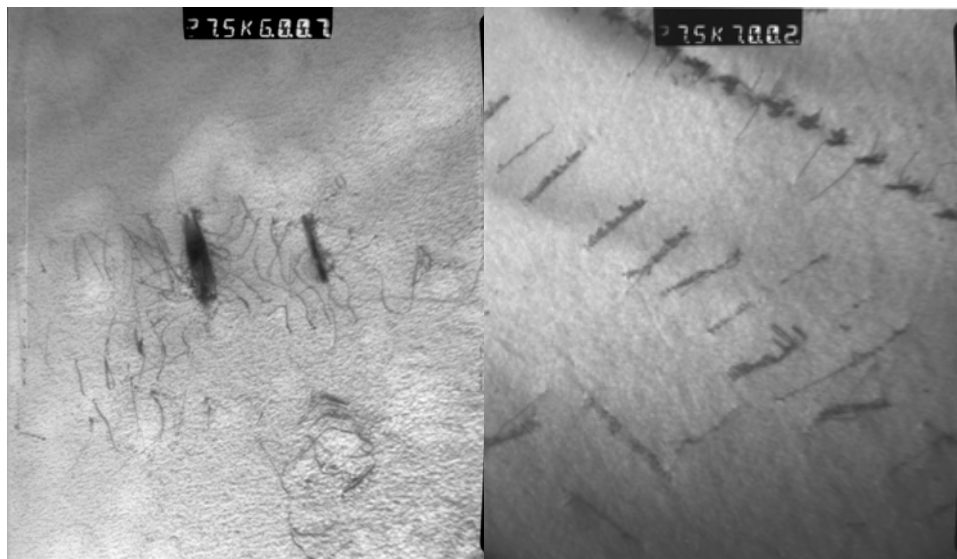


**Figure 7.6:** Electron microscope images of dislocation microstructures formed in pure iron deformed at elevated temperatures. Left: dislocation microstructure of iron deformed at 530° C, right: dislocation microstructure of iron deformed at 713° C. Note the more compact structure of pile-ups formed at the higher temperature (images courtesy of Z Yao and M L Jenkins, University of Oxford)

### 7.3 ACTIVATION DATA AND MODELLING

Modelling of the activation resulting from irradiation of materials in the neutron fluences experienced in current and future fusion devices is carried out by an inventory code such as FISPACT. This requires large amounts of nuclear data; both cross sections and decay properties of nuclides as input. Maintaining and developing the nuclear data stored in the European Activation File (EAF) is a major task which has in the past been funded by EFDA, but in the future this responsibility will be taken over by F4E. During this transition period we have undertaken several ‘infrastructure’ improvements in preparation for the production

of the next version of the European Activation System (EASY) which is expected in 2010.

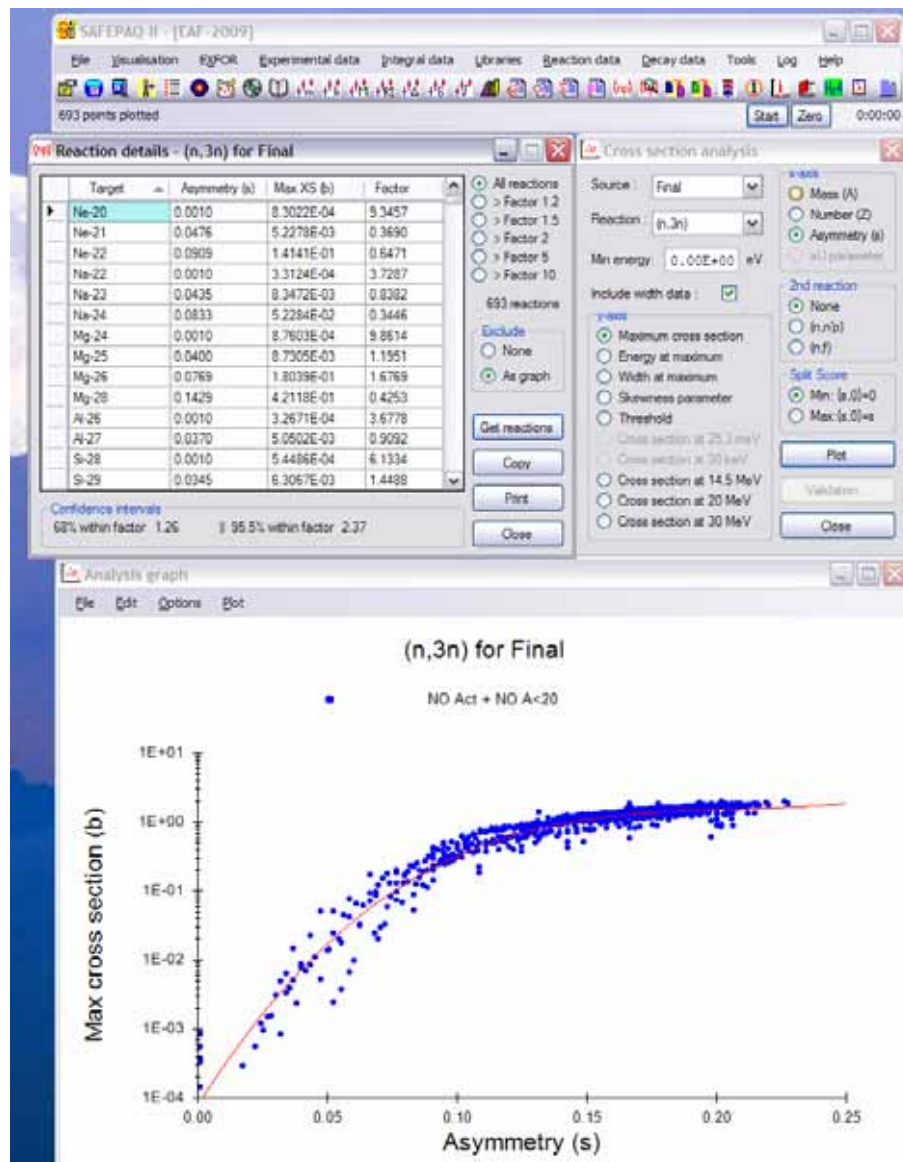


Figure 7.7: New version of SAFEPAC-II used for statistical analysis of (n,3n) reactions

The SAFEPAC-II application is used to store, visualise and process all the various sources of data which are selected and combined to form the EAF library. This application is about ten years old and it was necessary to rewrite this using the new version of Visual Basic. This ensures that continued development of this application will be possible in the future. Figure 7.7 shows SAFEPAC-II with windows open for a Statistical analysis of (n,3n) reactions.

The FISPACT code is also rather ancient and this is currently being re-engineered in FORTRAN-95 with modern algorithms and the need for fewer approximations. This will ensure that Culham remains at the forefront of this technology field.

The new version of the Activation Handbook has been completed. This extensive document (~660 pages) contains comprehensive graphical and tabular results for activation of all the stable elements in five fusion neutron spectra. This enables designers to readily determine activation properties of materials without running codes. The set of Importance diagrams for each element also enables all the

dominant radio-nuclides and the important reactions to be identified. It was found that only 923 out of the total of 2,231 nuclides are sufficient to completely describe the activation properties of all elements. Similarly only 5,105 out of the total of 65,565 reactions are important in producing these radionuclides at energies up to 60 MeV. By focusing future improvement efforts on subsets of nuclides and reactions, EAF library development will be made more efficient. Figure 7.8 shows the activity importance diagram for irradiated nickel. In each of the regions labelled by a nuclide, the nuclide is responsible for more than 50% of the activity. It can thus be seen which nuclides dominate at various decay times and for particular neutron energies.

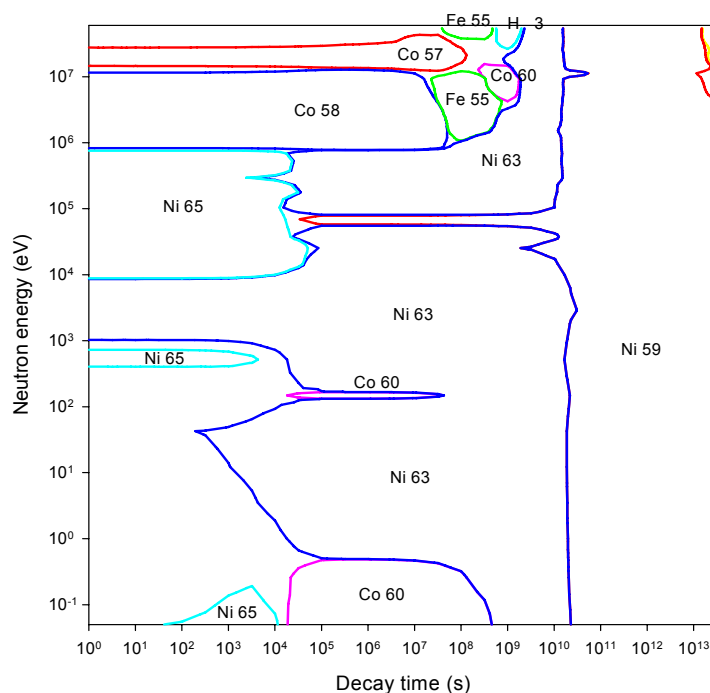


**Figure 7.8:** Activity importance diagram for irradiation of cobalt by neutrons for five years. The labelled regions indicate that within that region the nuclide contributes > 50% of the total activity following irradiation

Details of which of the various reaction types feature most frequently as the most important reactions are also presented in the Activation Handbook. The standard reaction types present in low energy libraries such as EAF-2003 are most common, for the 1,387 most important reactions only 71 are 'exotic' reactions such as (n,5n) 24 cases, (n,6n) 12 cases and (n, $\alpha$ ) 8 cases. It is fortunate that exotic reactions do not feature strongly as few of them have been measured and the predictability of the models codes is still rather poor for reactions emitting multiple particles.

A major area of work in the production of the next EAF library will focus on the improvement of the uncertainties for the cross sections. This will involve use of model code calculations using Monte Carlo sampling of parameters to give uncertainty data in many more groups than the four currently used. In addition an extensive review of available experimental data has been undertaken to improve the uncertainty database.

## 7.4 PLASMA-FACING MATERIALS IN JET

Our work on this topic as part of EFDA-JET Task Forces, previously covered mainly by the JET Science Area (Chapter 4), was moved to be jointly managed with other materials research in 2008/09. The main thrusts of the 2008/09 programme are given below.

JET will be fitted with a beryllium (Be) main chamber wall and tungsten (W) divertor in 2010 as part of the ITER-like Wall Project (ILW), to test out operational scenarios for ITER. However, power load calculations indicate that under certain operating conditions the flux to some areas of the wall may be too large for Be tiles. These areas include the neutral beam (NB) shine-through regions and tiles installed near the beam ducts (in the ports through which the beams enter the torus) to protect from NB re-ionisation. The ILW plans to use W-coated carbon-fibre reinforced carbon (CFC) tiles in these areas. However, erosion has never been measured in these areas, so W-coated CFC tiles were installed in each of these areas during the 2004/05 shutdown, and removed in 2007 for analysis.

The shine-through areas in JET include some of the Inner Wall Guard Limiter (IWGL) tiles, and some of the recessed areas between limiters where there are Inner Wall Cladding tiles. Tiles on the JET IWGL limiters are mounted in pairs - left (L) and right (R) - and there are 18 pairs per limiter numbered from top (1) to bottom (18). Two tiles were coated from the limiter in sector 7Z - one near the bottom (7Z17R), the other near the centre (7Z12L), though each should receive similar fluxes during NB heating. Each tile had one half (poloidally) coated with  $\sim 3 \mu\text{m}$  W and the other half with  $\sim 3 \mu\text{m}$  rhenium (Re).

After exposure in JET, the coating on one of the two IWGL tiles from the beam shine-through region (7Z17R) was shown by Ion Beam Analysis (IBA) to be similar to the original  $3 \mu\text{m}$  thickness. However, on the other tile the coating has been completely eroded over a toroidal width of  $\sim 70 \text{ mm}$  where the tile is closest to the plasma boundary. As can be seen in Figure 7.9, as the tile curves further from the boundary into the scrape-off layer (SOL) some remaining coating is seen, and then this coating is covered with a layer of deposit; the situation is shown schematically in Figure 7.10. The integrated energy densities to tiles 7Z12L and 7Z17R during the divertor phases for the  $\sim 3,500$  discharges were similar at  $\sim 5,300$  and  $\sim 4,700 \text{ MJm}^{-2}$ , respectively, with peak power densities of  $7.5$  and  $6.5 \text{ MWm}^{-2}$ . Furthermore any shine-through effect would be uniform over each tile and not related to distance from the edge of the main plasma, the last closed flux surface (LCFS). Thus the differences between the two tiles cannot be attributed to shine-through or plasma loading during the divertor phase. However, this transition from a region of erosion to one of deposition is clearly characteristic of a plasma limiter. The plasma in JET normally starts in contact with the outer limiter, but is then moved to be in contact with the inner wall (i.e. IWGL) when the plasma is still reasonably circular during the initial 'ramp-up' period, which varies in length from  $\sim 1$ - $10 \text{ s}$ , when the full performance plasma is created. In this period the LCFS will be at the IWGL surface, with ion temperatures typically  $50$ - $200 \text{ eV}$  and incident ion energies three times that for deuterium, together with a significant impurity (carbon) concentration giving potentially several times increased energy. Thus erosion on tile 7Z12L is far more dramatic than at any point in the divertor - the W (and Re) coatings are completely stripped from the plasma-exposed surface for a distance of  $\sim 10 \text{ mm}$  into the SOL from the leading edge of the tile (Figure 7.10). The plasma will also be in contact with the adjacent tile 11, and a marker stripe in this position was similarly stripped during the 2001-04 JET campaigns. By comparison, the leading edge of tile 17 is already much more than  $10 \text{ mm}$  from the LCFS during this phase so the coatings are not eroded.

A major objective of the ILW is to study operations without significant amounts of carbon in the plasma, so erosion of carbon from shine-through tiles is unacceptable. Thus as a result of this experiment, the W-coated shine-through tiles for the ILW will be set at least 20 mm behind the other (Be) inner wall limiters. No erosion was observed on the tiles installed near the beam ducts to protect from NB re-ionisation, so these will be coated as planned for the ILW.



**Figure 7.9:** Photograph of tile 7X12L installed near the midplane of an Inner Wall Guard Limiter after exposure in JET 2004-07. Coatings of W and Re visible at the left of the tile have been totally eroded towards the right of the image

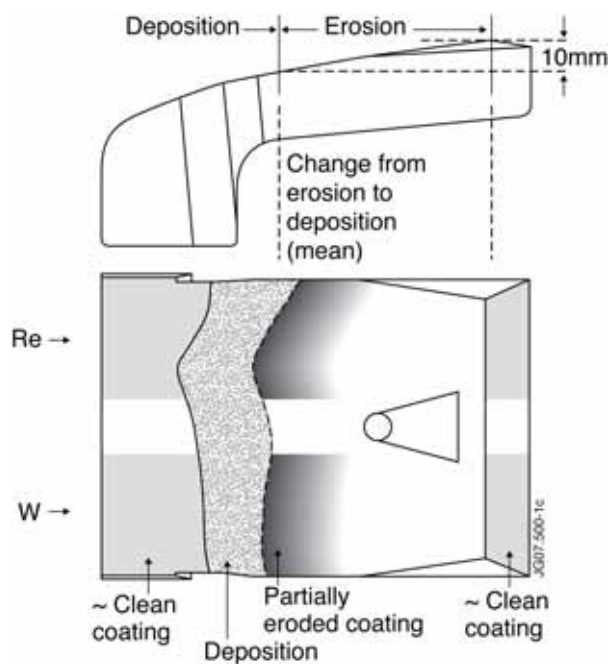


**Figure 7.10:** Schematic of the tile 7X12L, and a side view, showing the regions of interest

Tiles are removed from JET at every shutdown for analysis, and the patterns of erosion/deposition and H-isotope retention are measured. Three different divertor structures have been employed since 1998 as shown in Figure 7.11; the latest (HD) divertor can also be used with plasma contact on tiles 1 and 5 rather than tiles 3 and 7 as shown. It is clear from the analysis of tiles removed in 2007 that there has been a change in the deposition pattern over recent divertor campaigns. Figure 7.12 shows the Be/C ratio along tile 6 – the inboard edge of tile 6 (adjacent to tile 5) is at s co-ordinate 1,321 mm and the outer edge is at 1,512 mm; the s co-ordinate is the distance along the tiles around the divertor cross-section. Values of Be/C are corrected for the different analysis depths for Be and C. It is clear from the figure that the Be/C ratio has greatly increased for recent campaigns; there has also been a systematic increase in the ratio on tile 4 at the inner divertor, though the absolute value is considerably lower. The positions of the peaks in the distribution of the tile 6 Be/C ratio data for the tiles removed in 2007 correlate with the most frequently-occurring strike zone positions in the 2005-07 campaigns. There has also been a change in the amounts of material being deposited in the areas of the divertor shadowed from direct interaction with the plasma (shown on Figure 7.11). In the earliest JET divertors, deposition was very asymmetric, with heavy deposition at the inner shadowed region, but negligible deposition at the outer region, and this was also true for the MkII Gas Box divertor, shown in Figure 7.11. However, for the MkII SRP divertor, there was some deposition also at the outer shadowed region, and for the MkII HD divertor the ratio between amounts deposited at the inner and outer corners of the divertor is less than a factor of two. Work is now in hand to provide explanations for these changing conditions in JET; among the parameters being explored are strike point positions and ELM behaviour, whilst other diagnostics such as surface temperatures and the spectroscopy of impurities are also being checked for systematic changes.

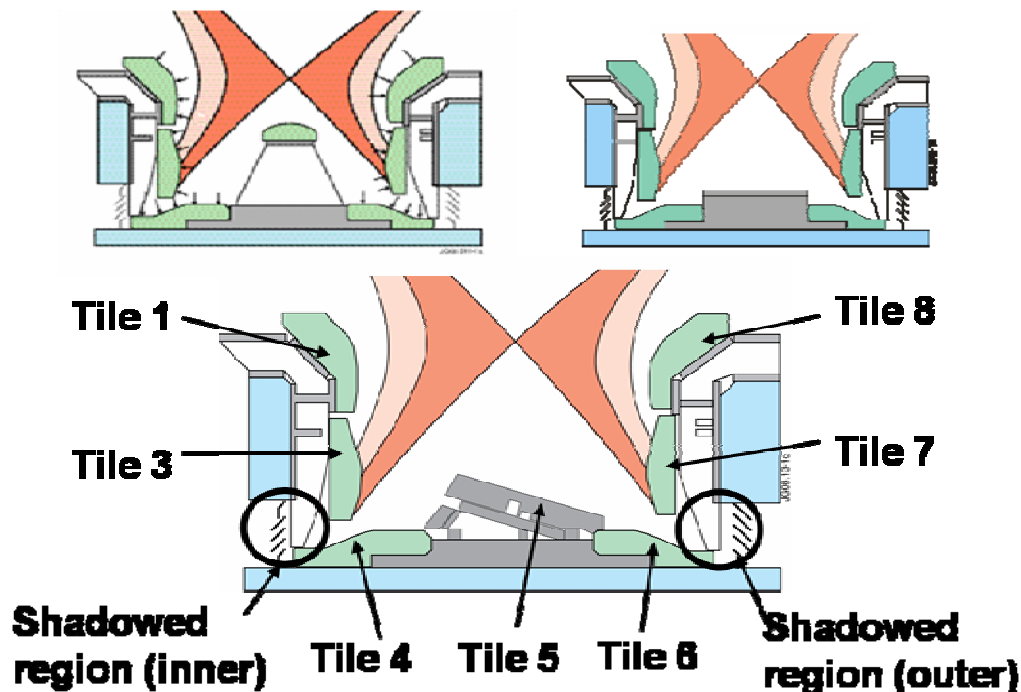


**Figure 7.11:** Divertor structures during the last three JET campaigns: top left Mk II Gas Box (1999-2001), top right MkII SRP (2001-04), bottom MkII HD (2004-07 - this divertor can also be used with plasma strike points on tile 1 and 5 rather than 3 and 7)

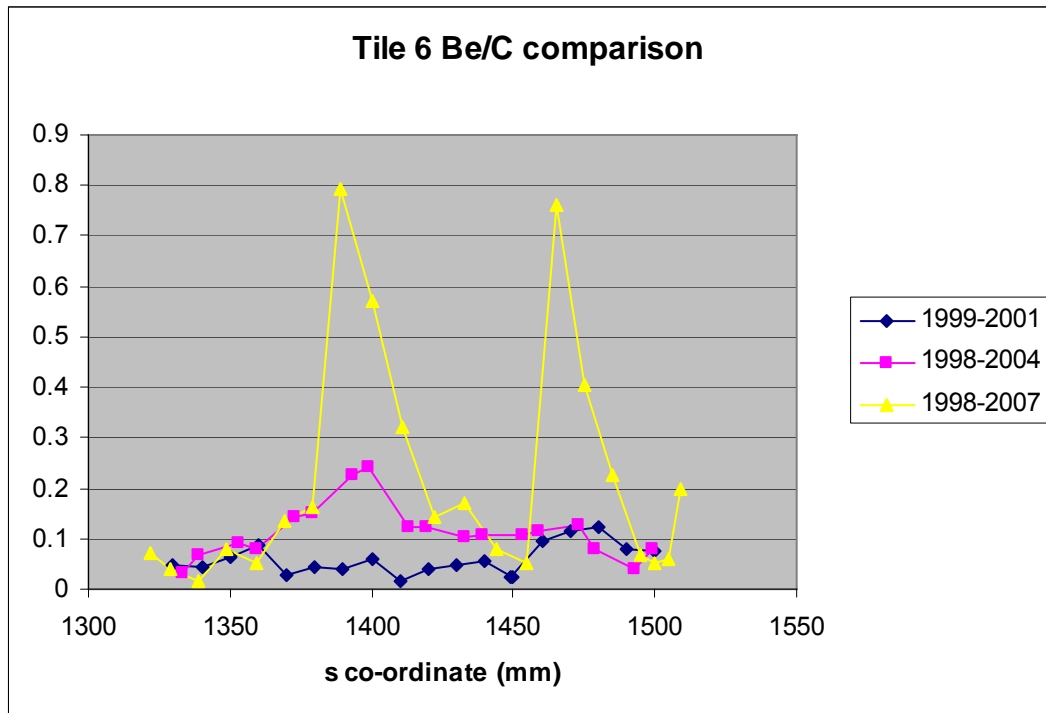


**Figure 7.12:** Comparison of Be/C ratios (corrected for analysis depth) on tile 6 for tiles removed after the last three JET campaigns (1999-2001 – Mk II Gas Box, 2001-04 – MkII SRP, 2004-07 – MkII HD divertors)

## 7.5 TECHNOLOGY

The UKAEA Association's Fusion Technology programme aims to promote the cost-effective accelerated development of fusion as a safe, environmentally benign and economically attractive source of energy. This is achieved through work on a number of 'fast track' and underlying technology issues.

Technology for ITER is covered in Chapter 8. Our other Technology work (including work for the EFDA and IEA programmes) is split into three sub-packages of work:

- systems studies, examining issues relating to DEMO and Power Plants, and the proposed Components Test Facility;
- socio-economic studies, assessing the role of Fusion power in a future energy economy;
- 'Technology Growth' aimed at growing the Fusion Technology work in the UK by outreach to Universities and other Research Institutes, with a possible programme of joint bids to EPSRC and other funding bodies to support Fusion Technology projects.

### 7.5.1 SYSTEMS STUDIES

#### A DEMO and Power Plant Conceptual Studies

Following earlier power plant studies and the approval of ITER, emphasis remains on considering the optimal route to developing fusion power, and in particular the options for a demonstration power plant (known as DEMO) to follow ITER.

Significant effort has gone into considering the possibilities for a DEMO device to be built relatively early, possibly before ITER has finished its operational phases.

Exactly how this impacts on the design of DEMO is an issue requiring both technical and strategic assessment, rather than being purely a technical question. Clearly DEMO lies somewhere between ITER and a full power station, and it seems natural to assume that the earlier DEMO is built, the closer it must be to ITER. The questions that naturally arise relate to where in this spectrum DEMO should lie and how that depends on the development time allowed before DEMO.

Firstly, the production of electricity in a modest performance device may imply that electricity production is the only target for the device, whereas it is more common to assume that a DEMO device must be a prototype for a power station, by establishing the operating mode for a power station and demonstrating the safety and environmental case for fusion. Certainly, these last two items should not be given up, but there is a danger in emphasising only the production of electricity, that there would still need to be another intermediate step before a real working power station could be constructed. This introduction of a further step would risk delaying rather than advancing fusion. The counter argument is that once fusion is demonstrated to produce electricity, industrial interest would be raised to a level where serious, rapid, development of a power plant could be pursued.

An example of where problems may arise can be found in some earlier DEMO design concepts, for instance some studies considered a device assumed to have a 1,000 s burn time. Although this could be used as a perfectly adequate demonstration of electricity production, it probably does not provide a good basis for a power station as it would imply almost one million pulses over a power plant life of 30 years – very unlikely to be acceptable due to cyclic fatigue. The issue of how close DEMO should be to a power station is a subject of ongoing debate, and the ongoing work on DEMO helps to inform that debate.

## **A1 Power levels**

It is common to consider fusion power plant concepts that produce net electrical power of 1 GW or more, because the cost efficiency of the plant improves with power output. For DEMO, however, this may not be as important and it may be preferable to produce a smaller, lower power device at lower capital cost. This could be particularly important in a first of a kind plant where (fusion specific) capital costs are likely to be dominant. Lower power levels may also lower other important features of the plant, such as the current drive power requirement in a steady state plant. On the other hand, a smaller device will tend to have a higher recirculating power fraction than a larger device, again influencing the discussion of how close to a power station DEMO should be. Studies have looked at the role of key parameters in influencing the steady-state current drive requirements. The main factors which can reduce the current drive power are reduced net electrical power and increased confinement enhancement (“H factor”). The explorations carried out suggest that a reasonable compromise for a steady state DEMO would target less than 1 GW, perhaps 0.75 GW, of net electrical power.

## **A2 Mode of operation – pulsed or steady state**

In power plant studies, the preferred mode of operation remains steady-state, using non-inductive means to maintain the plasma current, both by the self-driven, bootstrap current, and by external heating and current drive schemes. These are the assumptions underlying most of the plant concepts studied in recent years. The alternative to this is to run a pulsed device with a pulse length sufficiently long that the power plant lifetime can reach values typical for the power industry, e.g. 30 years, with an energy storage system to smooth out the (short) down time between power pulses.

These alternatives have been explored in more detail and analysis shows that a pulsed device tends to be more expensive than a steady-state device (Figure 7.13), both because cyclic stresses reduce the performance and because a large solenoidal coil is needed to maintain a long pulse length, increasing the machine size. Although partial current drive can be used to increase the pulse length in a smaller machine, such a device is still larger than a steady-state device, and has the additional feature of needing a reliable current drive system, similar to the steady-state version.

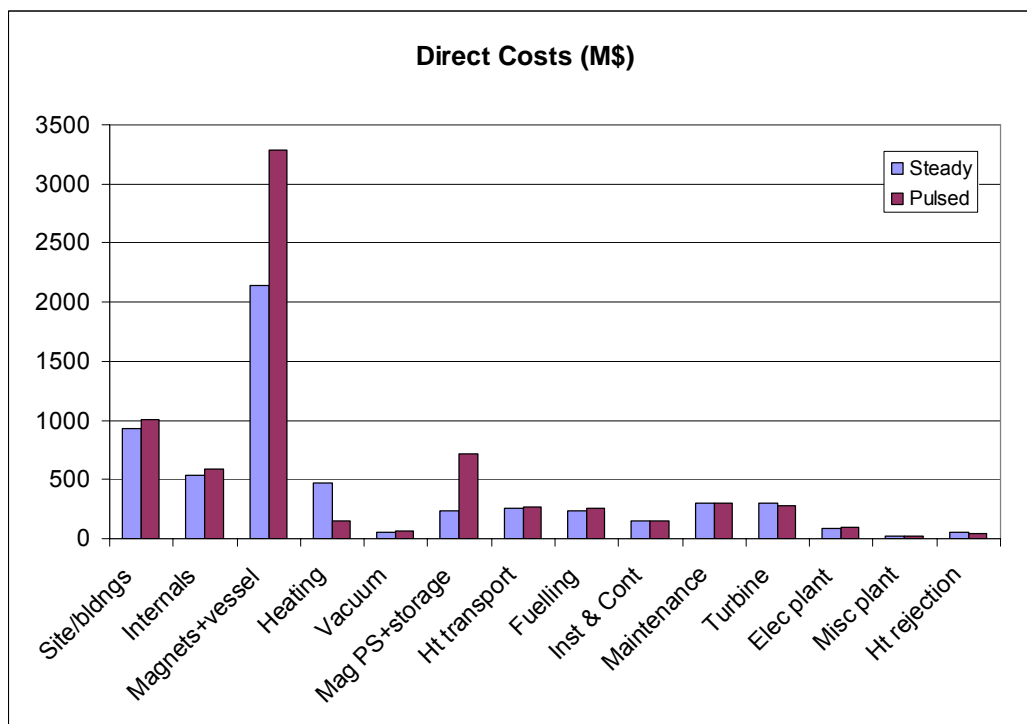


Figure 7.13: Cost comparison of a pulsed and a steady-state fusion power plant

The foregoing discussion has concentrated on how DEMO can be a prototype power station, but it may be possible to relax some of the assumptions. For instance, an early DEMO is highly unlikely to have high availability in its early phase of operation so the lifetime number of pulses, and the materials damage from neutrons, that the plant must tolerate is likely to be lower than assumed for a power plant. For instance, if DEMO needs to survive for 20 years and has an average availability of around 50% over that time, it may be acceptable to run 30,000 pulses of around three hours duration, considerably reducing the plant requirements. Even though this runs the risk of not demonstrating the true conditions needed for a power plant, the possibility of DEMO targeting lower power output and also reduced performance in terms of lifetime pulses is something that should be discussed and explored further, as an extension to this work.

### A3 Tritium generation

One of the most important functions of a DEMO device, and crucially one that will not be fully tested by ITER, is self-sufficiency in tritium. The blanket must produce slightly more tritium than is consumed in the plant, as it is impractical to supply the required tritium externally. As an indication, a 1 GW electric plant would need perhaps 100 kg of tritium per year, which exceeds the total known world supply of available tritium – much of which in any case is expected to be used in ITER. Whilst it may be possible to supply externally a total of around 10 kg over

DEMO's lifetime, this is only 1% of the tritium that DEMO would be expected to consume. Tritium generation is therefore crucial for a DEMO device.

As part of the DEMO studies, generic neutronics calculations have been carried out, particularly considering the generation of tritium. The calculations show the importance of the different factors in moving from 1-D (illustrated in Figure 7.14) to 2-D to 3-D calculations, with the tritium breeding ratio reducing as more realistic loss mechanisms enter the model. Although the solid blanket (HCPB) and lithium lead blanket (HCLL) achieve further ratios of 1.6-1.8 when enrichment of Li6 is used, this reduces to 1.1-1.2 in 2-D, with further reductions expected in 3-D which remain to be explored in detail.

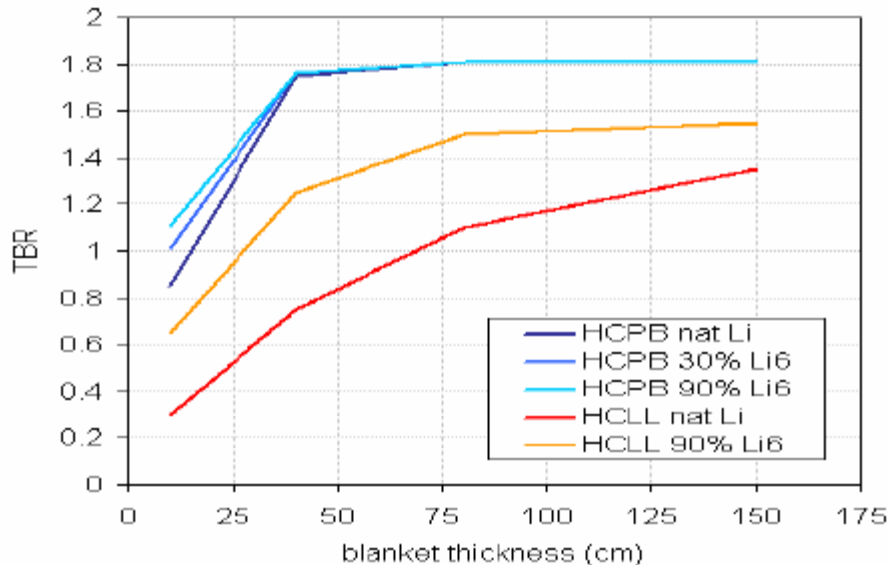


**Figure 7.14:** Example of 1-D calculations of the tritium breeding ratio for varying design and thickness of fusion blanket

Overall, it appears that the EU test blanket technologies to be trialled on ITER are capable of producing enough tritium to make a DEMO plant self-sufficient in tritium. There remains the possibility that a large number of ports, for instance for current drive in a steady state DEMO, could reduce the value excessively, however it is also the case that tritium generation behind the divertor modules is not included in this study. The effect of losses in heating ports and possible gains in blankets behind the divertor, as well as a more careful study of the effect of different material choices, are important features that are identified for further exploration.

#### A4 Summary on DEMO

Scoping studies of an early DEMO (EDEM0) have been carried out. A range of technical analysis, from systems studies to neutronics, has been completed and shows the way that an early DEMO design depends on the main assumptions. In carrying out these studies, we have also improved UKAEA capabilities in key areas needed for future, more detailed, DEMO studies.

There are clear advantages in a steady-state device, if it can be successfully built, however the potential simplification of removing the need for current drive is a clear advantage. This judgement depends to a large extent on whether DEMO must be prototypical of a power station – it would obviously be easier to demonstrate electricity production in a pulsed device if we were not concerned with fatigue life of the plant or the resulting cost of electricity.

The most important questions for DEMO are not only of a technical nature. Where it should lie in the range between ITER and a full power station is a matter of judgement, though if it falls too close to ITER then another intermediate step could be required, possibly delaying rather than advancing fusion power. The danger of delaying fusion would be exacerbated if the need to design DEMO at the same time as constructing ITER should distract from the timely delivery of ITER, because of insufficient resources in the fusion programme. On the other hand, if there were an international DEMO programme which included a range of facilities, an early DEMO could certainly be considered as an option for one of those facilities. The decision of whether an early DEMO should primarily demonstrate the production of electricity, or whether it must also be prototypical of a full power station remains key, and is an area for much ongoing work.

In the light of the crucial importance of these questions surrounding DEMO, for the future of the fusion programme, a new area of work has been started at Culham looking in more detail at the scientific and technical detail of the facilities and development programme needed to achieve fusion power. New and more detailed work on DEMO has begun whilst work on a Component Test Facility and materials development is ongoing. This new area of work will make up an increasingly important part of our future activities, whilst at the same time being integrated in, and contributing to, the collaborative work in this area co-ordinated by EFDA.

#### A5 Coupled materials and power plant work

There is a danger in fusion materials development of divorcing the materials programme from the fusion programme, for instance designing fusion power plant concepts around fusion data then using that to specify the properties that the materials must achieve. In fact, materials properties should be used as inputs to power plant studies, as well as using power plant studies to derive ultimate targets for the materials programme. Coupled analysis of this sort gives different insights into the coupling between materials performance and economic performance of fusion. The example of structural materials with low tolerable blanket fluence shows that larger machines can be the economic optimum, when plant availability is properly taken into account.

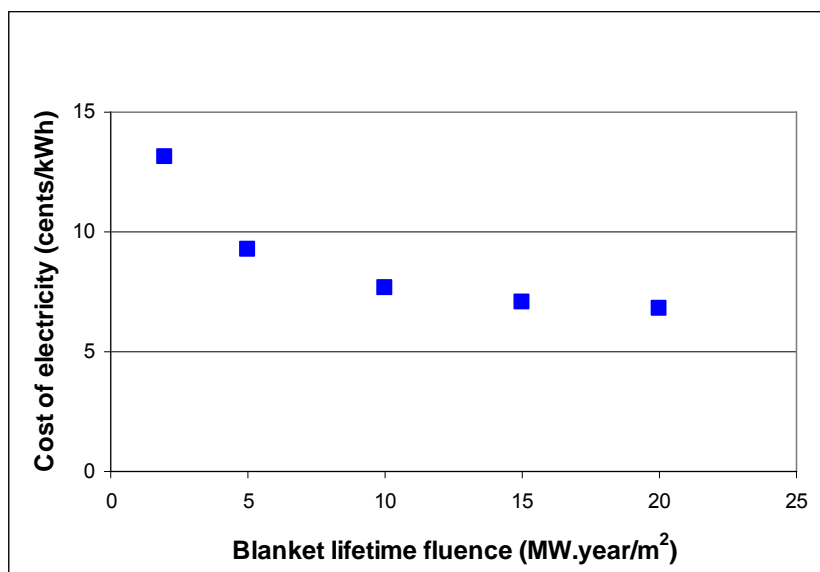


**Figure 7.15:** Cost of electricity variation with the assumed blanket fluence (quoted here in MW years per m<sup>2</sup>; for steel 1 MW year/m<sup>2</sup> corresponds approximately to 10 dpa)

The question of what targets we should aim for in the materials development programme, and how to interpret those targets from an economic perspective, is obviously complex. In particular, the target of around 150 dpa for fusion steels which is often quoted as a target, should not be seen as the minimum value necessary for fusion to be realised but, in coupled studies, emerges more as a maximum level beyond which there is little further benefit. Conversely, the role of fusion in the future energy market may depend critically on costs so even relatively small changes in fusion costs may have a substantial impact on future market share.

Research is presently at the point where advances in materials properties may substantially reduce fusion costs, for instance if a material with an operating limit of 20 dpa were improved to reach a level of 100 dpa, cost of electricity estimates would fall by around 60%, largely as a result of increasing availability.

Although the effect of reduced materials properties can be, to some extent, ameliorated by design, materials research remains an absolutely crucial part of producing an economically competitive energy system. The materials development work should be more integrated into power plant designs and the wider fusion programme, in order to optimise the fusion development programme as a whole.

## B Component Test Facility

The conceptual design of a Component Test Facility (CTF), based on the spherical tokamak, has been developed further. This device would produce simultaneously the neutron, particle and heat fluxes necessary to effectively test and optimise blanket modules, first wall structures and other components under the required fusion power plant conditions. Recent work has focussed on the divertor and start-up options

### B1 Divertor

The expanded divertor concept (also known as 'Super-X') has been applied to CTF. Here additional poloidal field (PF) coils allow the outboard divertor leg to extend radially outwards. This increases the radius of the target and allows much higher radiative heat loss from the long divertor leg. However, it does require at least one PF coil to be located inside the main vessel which raises maintenance and radiation damage issues. A cross section through the CTF is shown in Figure 7.16. Here the left hand side shows the previous compact divertor design while the right hand side shows a possible layout of the expanded divertor.

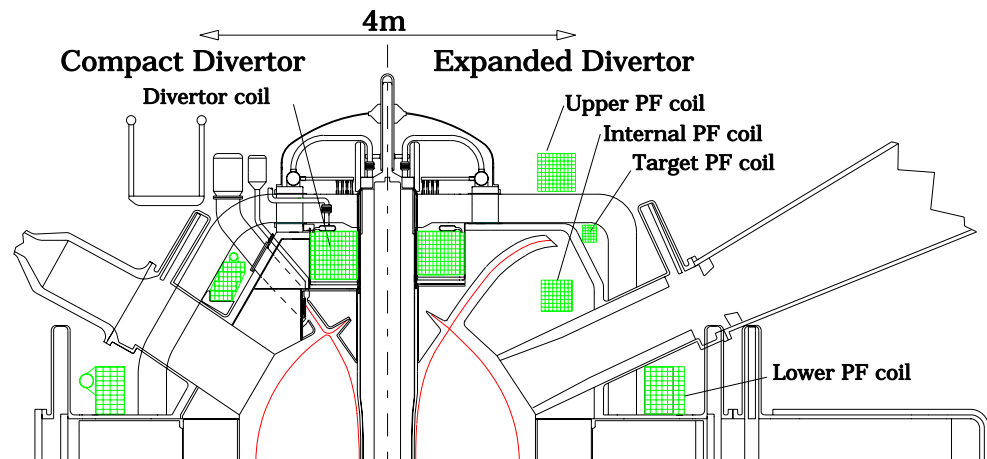


Figure 7.16: CTF cross section – LHS = Compact divertor, RHS = Expanded divertor

In order to accommodate the expanded divertor the corners of the load assembly are now fully utilised. However, since the internal PF coil can not be easily replaced it must have a predicted life of the full time span of the CTF which is about 12 years. This requires effective neutron and gamma radiation shielding around this coil to protect the cyanate ester resin insulation between its turns. The radiation damage has been analysed using the MCNP neutron and photon transport code and a number of shielding options have been explored including boronated steel, tungsten carbide and boron carbide. The results showed that all the coils can be adequately shielded provided that the internal PF coil is protected by a composite shield using one or more of the above materials. The 3D model used for the neutronic analysis is shown in Figure 7.17.

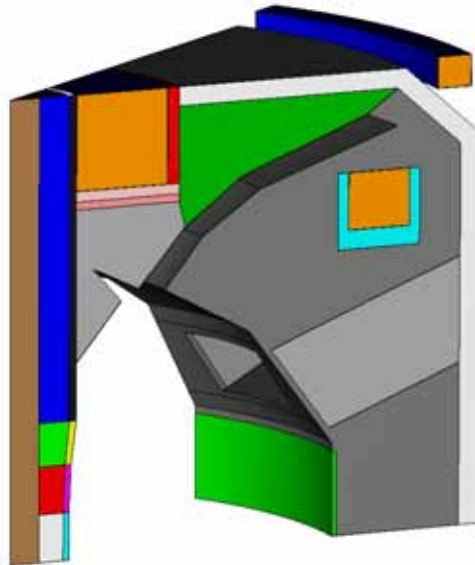


Figure 7.17: 3D neutronics analysis model of one sector of CTF

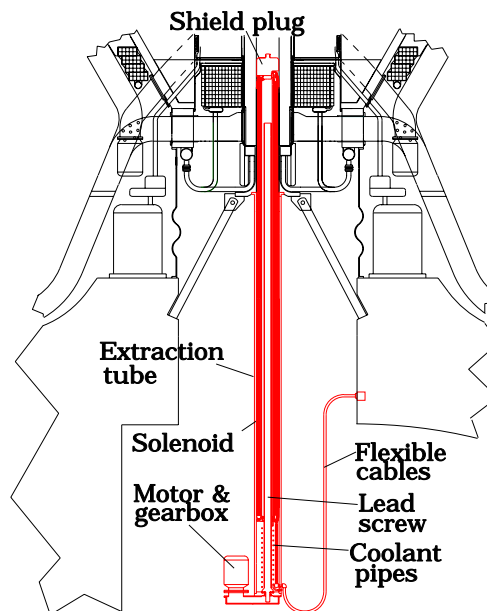


Figure 7.18: Start-up solenoid retracted beneath CTF

## B2 Start-up options

The start-up of the CTF has also been developed further. A method which does not rely on a permanent solenoid around the centre column is needed, as there is insufficient space for a neutron shield for this component. An attractive start-up

scheme is to use a retractable start-up solenoid located inside the central hole of the centre rod. The uni-directional flux swing from this coil is expected to develop an initial plasma current of  $> 0.5$  MA. The plasma would then be ramped up to its full value of about 6 MA by the combination of neutral beam injection and flux swing from the ramp-up of the external PF coils. In order to prevent toroidal currents being induced in the centre rod which would cancel out the flux from the solenoid, the rod is segmented using expanded graphite layers between the copper segments to increase its toroidal resistance. The retractable solenoid is shown in its fully extracted position under the main CTF device in Figure 7.18.

### 7.5.2 SOCIO-ECONOMIC STUDIES

As part of the assessment of the possible role for fusion in a future energy market, a new economic-energy-energy model, known as the EFDA/TIMES model has been prepared by EFDA and its partners, including UKAEA. As input to this study, a range of assessments of the expected economic performance of fusion power plants, assuming they are successfully developed, have been reviewed and interpreted to give inputs to the model. Essentially, fusion is represented as two technologies, each with two vintages associated with the level of maturity of the plant. Figure 7.19 shows examples of a range of studies, including the data proposed for the EFDA/TIMES model, shown in the last four columns.

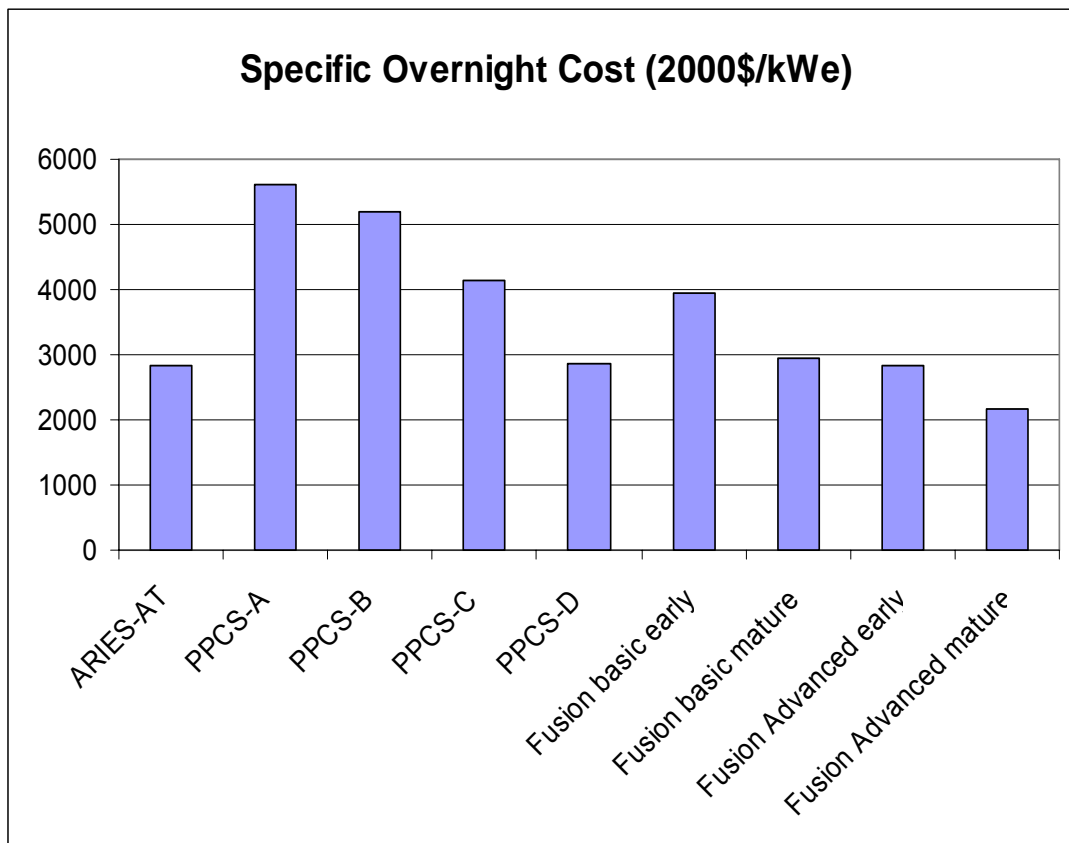


**Figure 7.19:** Cost comparisons of a range of fusion studies

This assessment, along with a range of other studies, has been used to derive a 'Fusion data sheet' which is proposed for use in energy scenario modelling. This is shown in Table 7.1 and will be revisited in the light of new concepts and progress, particularly as a result of the conclusions from the ongoing DEMO studies.

	Date	Specific capital	Efficiency	FIXOM	VAROM
Basic plant	2050	3,940 \$/kW	42%	65.8 M\$/GWa	2.16M\$/PJ
	2060	2,950 \$/kW	42%	65.8 M\$/GWa	1.64M\$/PJ
Advanced plant	2070	2,820 \$/kW	60%	65.3 M\$/GWa	2.14M\$/PJ
	2080	2,170 \$/kW	60%	65.3 M\$/GWa	1.64M\$/PJ

**Table 7.1:** Fusion Data Sheet, derived from Power Plant Conceptual Study (PPCS) reports modified in the light of DEMO studies, intended to provide economic data for use in wider energy modelling. Notes on the table:

- costs are in year-2000 US \$ (fixom and varom are fixed and variable operating and maintenance costs);
- capital costs are overnight costs, neglecting interest during construction;
- decommissioning costs are included in fixom, waste disposal is included in varom;
- tritium generating material is lithium lead with 90%  $Lf^6$  enrichment;
- the vintaging shown for each model in the table reflects “early technology” (10<sup>th</sup> of a kind) and ‘mature technology’ (100<sup>th</sup> of a kind). The associated learning factors (applied to the fusion costs only) are 0.5 and 0.25 leading to total plant costs which are reduced from a first of a kind by 36% (for 10<sup>th</sup> of a kind) and 52% (for 100<sup>th</sup> of a kind). This represents a progress ratio for the whole plant of approximately 0.9;
- a maximum bound on capacity growth of 26% per annum is recommended for fusion (which is the basis of the assumed learning of timescale for the capital costs in the table above). However, future modelling of the energy market should not be restricted to this assumption. A range of bounds should be considered feasible, and maximum bounds of 26-40% cannot be ruled out as long as the increased costs of rapid expansion can be taken into account.

Although the EFDA/TIMES model is still being modified, to correct errors, incorporate updated information, and reflect comparisons with other data sources, the early version of the model was used, incorporating the fusion data sheet, for a provisional assessment of the potential role for fusion in the future energy market. Although this may change in the light of modifications, the early results are as shown in Figure 7.20 which shows the potential main contributors to the global electricity market by 2100. The largest contributions in these scenarios come from coal, nuclear fission, nuclear fusion and wind power, although coal is essentially excluded if there is a carbon constraint. Other sources such as coal with carbon capture and storage, and solar PV are allowed in the model, but remain too expensive to be used. The main points of interest here are that fusion can play a role, on the basis of the information in the fusion data sheet, and that the role is quite price sensitive, since changing fusion prices by 20% changes fusion’s market share by around 50%. As usual in this sort of modelling, it must be emphasised that these are not predictions of the future but scenarios that allow the user to explore the effect of different assumptions on the possible outcome.

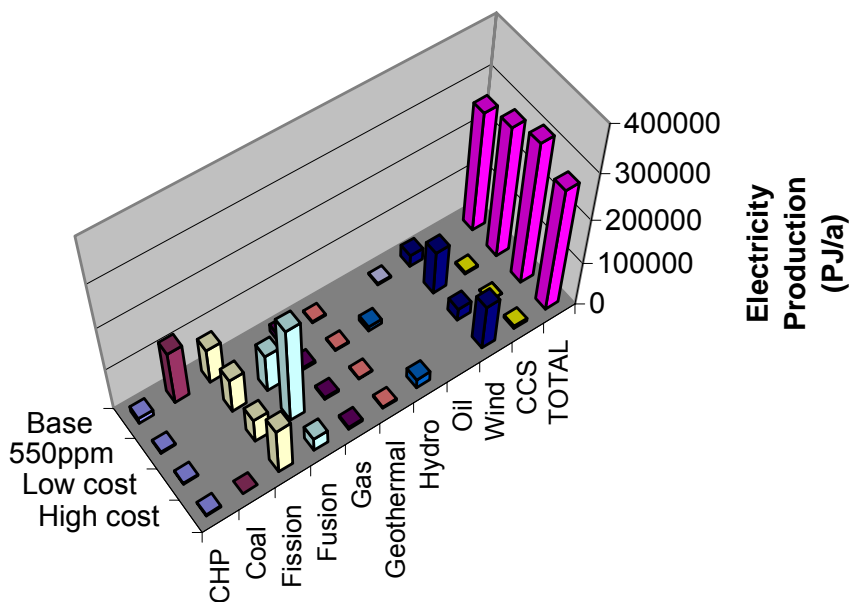


**Figure 7.20:** Results for electricity production by source in 4 scenarios; Base has no carbon constraint; 550 ppm restricts the atmospheric CO<sub>2</sub> to that concentration; low cost and high cost applies to a 20% reduction and increase, respectively, in fusion's costs

### 7.5.3 TECHNOLOGY GROWTH

In 2008/09 UKAEA Culham began a series of discussions with university groupings, and other research institutions on technology issues and the possibility of co-operation. The first of these discussions to yield fruit was on the development of Negative Ion Sources, which are of use both in fusion and industrial applications. In April 2008 UKAEA, Glasgow University, Queen's University Belfast, Heriot-Watt University and the Open University (OU) agreed the content of a joint proposal to be submitted to EPSRC (the UK Research Council that *inter alia* funds engineering, physics and fusion), with each party taking responsibility for a single work package and OU acting as the leading establishment. The proposal aims to establish improved negative ion sources both for fusion and industry. This may be by the use of alternative materials, improved design arising from greater understanding of the formation and transport mechanisms or novel processes. In July 2008 the Outline Proposal was submitted to EPSRC for consideration under the Programme Grant scheme. This outline proposal was accepted by EPSRC and the consortium submitted a full proposal in October 2008. It was subsequently decided that the proposal would be better targeted at a 'Managed Programme' Grant, these being better suited to strategic development. A submission to the Managed Programmes of EPSRC was made in January 2009, and will be assessed in summer 2009.

Other discussions for programme grant applications are in train with Imperial College and Rutherford Appleton Laboratory on "Technologies Underpinning Fusion". Culham have also had preliminary discussions with the Dalton Institute at Manchester University.